

Probing the Interactions of O₂ with Small Gold Cluster Au_n^Q (n = 2–10, Q = 0, –1): A Neutral Chemisorbed Complex Au₅O₂ Cluster Predicted

Hong Xiao Shi,^{†,‡} Wei Guo Sun,[†] Xiao Yu Kuang,^{*,†,‡} Cheng Lu,^{*,†,§} Xin Xin Xia,[†] Bo Le Chen,[†] and Andreas Hermann^{*,||}

[†]Institute of Atomic and Molecular Physics, Sichuan University, Chengdu 610065, China

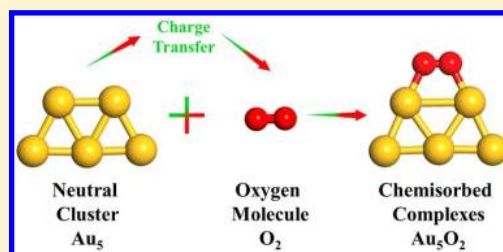
[‡]Department of Physics, Nanyang Normal University, Nanyang 473061, China

[§]Department of Physics and High Pressure Science and Engineering Center, University of Nevada, Las Vegas, Nevada 89154, United States

^{||}Centre for Science at Extreme Conditions and SUPA, School of Physics and Astronomy, The University of Edinburgh, Edinburgh EH9 3JZ, United Kingdom

Supporting Information

ABSTRACT: Enormous progress has been made in catalytic oxidation reactions involving nanosized gold particles. However, the reaction mechanism of O₂ with neutral gold clusters remains complicated. Here, we have performed an unbiased structure search for Au_n^Q and Au_nO₂^Q (n = 2–10, Q = 0, –1) clusters by means of CALYPSO structure searching method. Subsequently, the lowest-energy candidate structures were fully optimized at the B3PW91/Au/LANL2DZ/O/6-311+G(d) level of theory to determine the global minimum structures. Based on the ground-state structures of Au_n[–] and Au_nO₂[–] (n = 2–10), we have simulated the photoelectron spectra (PES) using time-dependent density functional theory. The good agreement between simulated PES and the corresponding experimental data suggest that the current ground-state structures are the true minima. The locally maximized value of the adsorption energy in Au₅O₂, where the unpaired electron of Au₅ can transfer to O₂, makes it the most promising candidate of the chemisorbed complex. A comprehensive analysis of molecular orbitals and chemical bonding of the Au₅O₂ cluster reveals that O₂ can be chemisorbed onto the neutral Au₅ cluster.



1. INTRODUCTION

As the noblest of all metals, gold has fascinated humankind since ancient times due to its enchanting color and chemical stability.^{1–5} In the extended state, gold does not, for instance, form any stable oxides at ambient conditions, though some have been proposed for low temperatures or high pressures.^{6,7} Added interest in gold has arisen because, different from the properties of bulk counterparts, gold at the nanometer scale possesses a rich array of new properties. Haruta et al. discovered that Au can express extraordinary catalytic activity when it is dispersed on certain catalyst supports.⁸ Subsequently, nanosized gold particles have been found to exhibit unusually strong catalytic capabilities in a wide variety of chemical reactions such as CO oxidation,^{9–11} propylene epoxidation,¹² water–gas shift,^{13,14} and hydrogenation of unsaturated hydrocarbons.¹⁵ Among these, CO oxidation catalyzed by nanosized gold particles has attracted considerable attention.

In the past decade, many experimental and theoretical studies of CO oxidation have been devoted to revealing the essence of the catalytic activity of Au nanoparticles.^{16–24} Haruta et al. suggest that CO reacts with molecularly adsorbed oxygen on gold catalysts to form carbonate species (CO₃[–]), which are

then converted to CO₂.²⁵ To reveal the catalytic mechanism of gold, it is therefore important to fundamentally understand the interaction of gold clusters with O₂. A systematic study of the interaction between Au_n[–] and O₂ supported by photoelectron spectroscopy calculations revealed that O₂ was chemisorbed to Au_n[–] clusters where n is an even number.²² Subsequently, the group of Wang determined there are two modes of O₂ activation by small even-sized Au_n[–] clusters: superoxo and peroxo chemisorption, with O₂ binding to Au_n[–] via one or both oxygen atoms.²³ Lee et al.²⁴ theoretically studied the geometrical and electronic characteristics of Au_nO₂[–] clusters (n = 2–7). Most of the theoretical studies have shown an even–odd alternation of several observables for anionic clusters, which is consistent with experimental reactivity observations. However, despite the enormous progress that has been made, the picture for the neutral clusters is still not entirely clear because of the shortage of direct experimental probes for the uncharged species. Then, theoretical studies are of paramount importance

Received: September 10, 2017

Revised: October 15, 2017

Published: October 18, 2017

for these systems. Landman et al. hold that neutral Au clusters are insufficient to activate molecular oxygen.²⁶ Jena and co-workers argued that, because of the high electronegativity of Au, electron transfer should take place from O₂ to Au₂ and Au₄ in the neutral Au₂O₂ and Au₄O₂ clusters.²⁷ Ab initio calculations support that neutral Au clusters can interact with O₂.^{28,29} Vibrational spectroscopy has been used to study O₂ adsorption on small neutral Au_n clusters, and it was concluded that adsorbed oxygen is activated due to charge transfer from the gold cluster.³⁰ Very recently, structural transformations of Au_n clusters upon O₂ adsorption have been surveyed computationally, focusing on isomerization and transition pathways.³¹ Clearly, more accurate theoretical calculations are needed to understand whether and how neutral gold clusters interact with oxygen molecules.

In order to explore the mechanism of oxygen adsorbed on neutral Au_n clusters, we have carried out a systematic study on small gold clusters. Here, we obtained the ground-state structures of Au_n^Q as well as Au_nO₂^Q (Q = 0, -1) clusters in the size range of n = 2–10 by employing the crystal structure analysis by particle swarm optimization (CALYPSO) method and density functional theory (DFT). In the first part of this work, we studied the ground state geometric structures of Au_n^Q and Au_nO₂^Q (n = 2–10, Q = 0, -1) clusters. For the anionic clusters, we simulated the PES of Au_n⁻ and Au_nO₂⁻ (n = 2–10) and compared them with experimental results. Subsequently, the inherent stability and the adsorption energy were calculated. On the basis of the calculated results, there is a promising candidate among the neutral Au_nO₂ clusters that can chemisorb oxygen particularly strongly. In order to gain further insight into the reaction mechanisms of the neutral species, detailed chemical bonding analysis is presented. Finally, we also explored the adsorption mechanism behind the electronic properties of neutral and anionic Au_nO₂ clusters and provide relevant information for unraveling the mechanistic details of CO catalysis by oxygenated gold clusters.

2. COMPUTATIONAL DETAILS

To identify the ground-state structures of Au_n^Q and Au_nO₂^Q (n = 2–10, Q = 0, -1) clusters, unbiased structure searches were carried out using the CALYPSO^{32–36} software, where a high search efficiency is achieved by implementing the PSO (particle swarm optimization) algorithm. The validity of this method in structure prediction has been certified by the successful identification of the structures in various systems, ranging from clusters to extended crystal structure.^{37–41} To predict low-lying isomers for each cluster size, we followed 50 generations of structures, where each generation contains 30 structures. Subsequently, the top 50 isomers are collected as candidates for the lowest energy structure and reoptimized using the Gaussian 09 package⁴² if within 5 eV among the initial candidate structures. Spin unrestricted density functional theory calculations with the B3PW91 functional^{43,44} are performed to reoptimize the geometries. The LANL2DZ⁴⁵ basis set was chosen as suitable for the gold atom and 6-311+G (d)⁴⁶ for the oxygen atom. Subsequently, frequency calculations were performed to verify the obtained structures were true minima on the potential energy surface. Different spin multiplicities, up to sextet and quintet for the neutral and anionic clusters, were considered in the geometry optimization process. We simulated the photoelectron spectra of the anionic Au_n and Au_nO₂ clusters using time-dependent density functional theory (TD-DFT).⁴⁷ The natural charges of oxygen molecule (NC(O₂)) were

calculated by natural bond orbital (NBO). Adaptive natural density partitioning (AdNDP)⁴⁸ bonding analyses were performed using the Multiwfn 3.3.8⁴⁹ program package, to gain further insight into the nature of the bonding.

3. RESULTS AND DISCUSSIONS

3.1. Geometric Structure. The ground-state structures of Au_n^Q and Au_nO₂^Q (n = 2–10, Q = 0, -1) clusters are exhibited in Figures 1 and 2, respectively, together with their low-lying

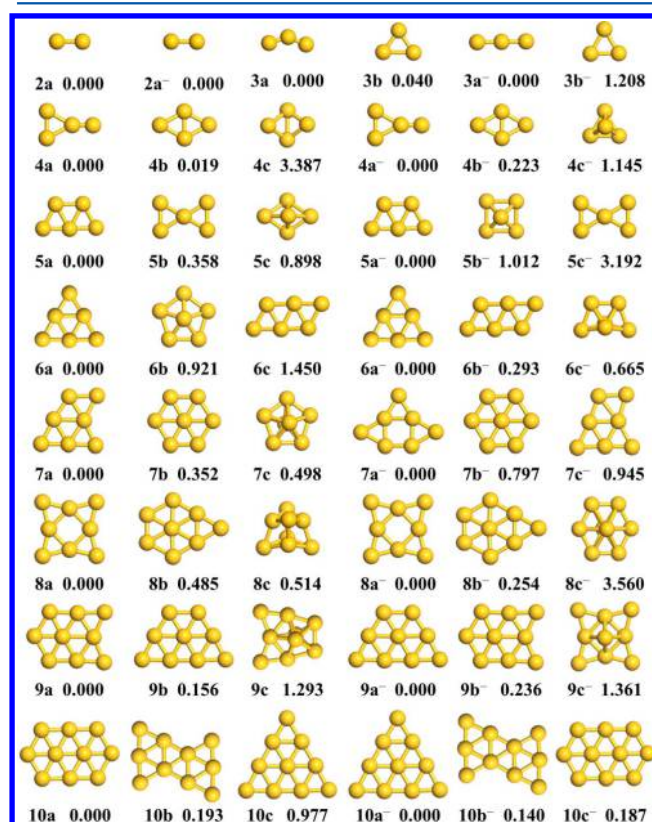


Figure 1. Optimized low-energy structures for Au_n^Q clusters (n = 2–10; Q = 0, -1). The ground state of the neutral and anionic clusters is labeled by “na” and “na⁻” for each n, respectively. The relative energies of each isomer are given in eV.

isomers. Each isomer of the neutral cluster is denoted by the label nx, where n stands for the number of gold atoms and x represents alphabetically the xth low-lying isomer of the cluster (e.g., “a” for the lowest energy isomer). Similarly, the anionic species are denoted by nx⁻.

As seen in Figure 1, pure gold clusters, whether neutral or anionic, all favor planar structures up to at least n = 10 in our work. This is due to strong hybridization of the atomic 5d and 6s orbitals of Au because of relativistic effects.^{50,51} The transition from 2D to 3D structures in gold clusters is debated in the computational literature, but a consensus seems to put the onset of 3D cluster structures around n = 11.^{52–61} The structures we find are in agreement with previous studies.^{62–64} The corresponding electronic states, symmetries, average binding energies E_b, and HOMO–LUMO energy gaps E_{gap} are summarized in Table S1 (see the Supporting Information). The ground-state structures of Au_n with n ≤ 8 have the same configurations for neutral and anionic clusters, except for Au₃ and Au₇, where the structures show some deformations due to the acquisition of an electron. Likewise, the acquisition of an

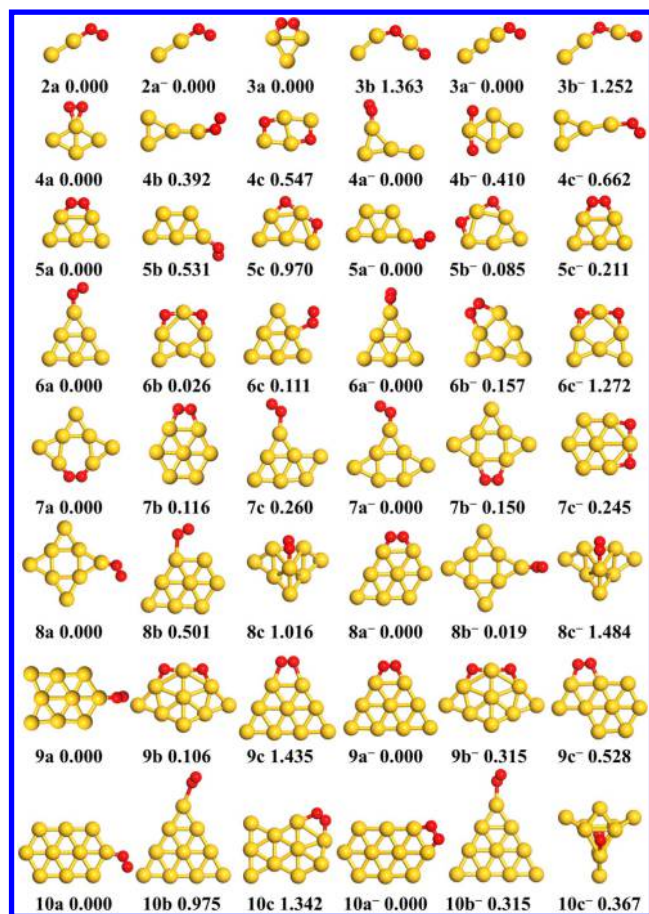


Figure 2. Optimized low-energy structures for Au_nO_2^Q clusters ($n = 2-10$; $Q = 0, -1$). The ground state of the neutral and anionic clusters is labeled by “na” and “na⁻” for each n , respectively. The relative energies of each isomer are given in eV. The red spheres represent oxygen atoms.

electron changes the energetic order for $\text{Au}_{9/10}$, switching 9a to 9b⁻ and 10a to 10c⁻ and vice versa. Similarly, the second-most stable structures nb are the same as those of nb⁻, for $n = 3, 4, 7, 8, \text{ and } 10$. Among the metastable structures, there are also some three-dimensional structures. As for the Au_nO_2^Q ($n = 2-10$, $Q = 0, -1$) clusters, in **Figure 2**, the ground-state structures are all quasi-planar geometries; that is, the Au atoms form a plane, and only the oxygen molecule potentially departs from the Au plane. We have also obtained some structures which contained two separate oxygen atoms and not an oxygen molecule; such structures are never the lowest-energy structure. This is not unexpected: the O–O bond is much stronger than the Au–O bond, so the oxygen molecule does not segregate and bind to multiple Au atoms. Note that only molecularly adsorbed oxygen on gold catalysts can react with CO to form carbonate species (CO_3^-), which are subsequently converted to CO_2 .²⁵ From now on, we only focus on structures that contain oxygen molecules. It is apparent that an oxygen molecule makes mainly two kinds of bonds with Au clusters (an exception is Au_4O_2 where both oxygen atoms are bonded to the same Au atom). In the first kind of bonding arrangement, O_2 forms a bent-triatomic unit with one Au atom (as in the 3a⁻ structure); in the other, O_2 binds to two Au atoms to form a cyclic structure (as in the 3a structure). This agrees with the conclusion reported by Mills et al.²⁹ and the classification by Pal et al.²³ The lowest-energy structures of Au_nO_2^- clusters ($n = 2, 4, 6$)

exhibit the former (superoxo) binding and $n = 8$ and 10 exhibit the latter (peroxo) binding motif. At the turnover point $n = 8$, the lowest-energy structure exhibits peroxo chemisorption, while the 8b⁻ isomer exhibits superoxo chemisorption. This phenomenon is consistent with the transition discussed by Pal and co-workers.²³ In the metastable structures 5c⁻, 6b⁻, and 7b⁻, the O_2 bonds to Au clusters in the same cyclic way as seen in 3a. In the ground-state structure of the $\text{Au}_{10}\text{O}_2^-$ cluster, the parent Au_{10}^- is not the global minimum D_{3h} isomer but the 10c⁻ structure; this agrees with earlier findings⁶⁵ that the low-lying isomers are reactive with O_2 and the global minimum can only form a physisorbed $\text{Au}_{10}(\text{O}_2)^-$ van der Waals complex. For the neutral Au_nO_2 clusters, if $n = 2, 4, 6, 8, 9, \text{ and } 10$, O_2 forms a bent-triatomic unit with one Au atom across all relevant structures, except for 9c and 10c. For the global minimum structures of Au_nO_2 ($n = 3, 5, 7$) clusters, O_2 binds to two Au atoms to form a cyclic structure. In particular, the ground-state structures 3a and 5a are of C_{2v} symmetry.

3.2. Photoelectron Spectra. In order to verify the accuracy of all of the ground-state configurations obtained in this work, the PES of the global minima of anionic Au_n^- as well as Au_nO_2^- clusters have been simulated using the TD-DFT method. The theoretical vertical detachment energies (VDEs) were obtained as the energy differences between the neutrals and anions both at the geometries of the anionic species. At the same time, the corresponding binding energy of the first peak position of the simulated PES represents the value of the VDE. The simulated spectra of the ground-state structures of anionic Au_n^- clusters are displayed in **Figure 3**, along with available

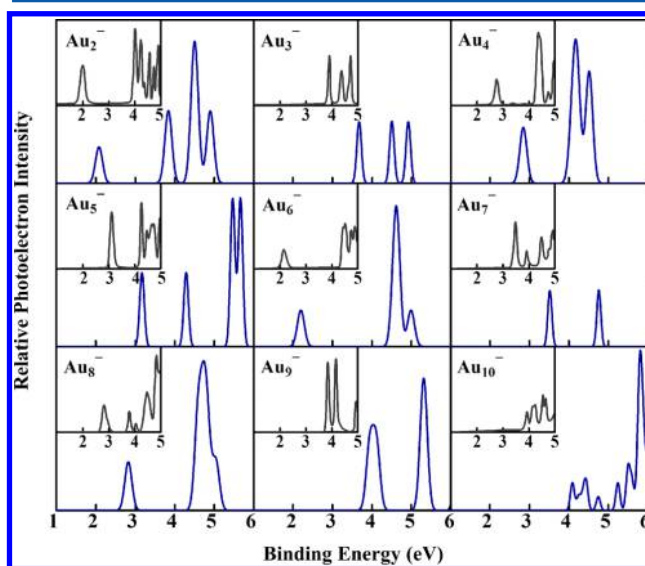


Figure 3. Calculated photoelectron spectra of Au_n^- ($n = 2-10$) clusters, together with the available experimental data⁶³ for comparison. The blue curves show the theoretical results, while the gray curves represent the experimental results.

experimental spectra⁶³ for comparison. Generally, the theoretical PESs of Au_n^- clusters are in agreement with the measurements. The simulated spectrum of Au_3^- shows three major peaks and fits well to the experimental result. For the Au_4^- cluster, there are three major peaks, and the third peak of the simulated spectrum corresponds to a weak shoulder of the experimental spectrum. As for the Au_6^- and Au_9^- , the positions of the simulated peaks are coincident with the experimental ones, disregarding splitting of the peaks. For $n = 2, 5, 7, \text{ and } 8$,

there are more peaks in the experimental spectra, but the first peaks are always in good agreement, which indicates that the ground-state structures we obtained are the true minima, while the experimental spectra might involve several isomers. As an important evaluation criterion of our theoretical results, the location of the first peak in the simulated PES is of particular importance, which represents a transition from the ground state of the anionic clusters to their neutral ground state ones. The theoretical as well as experimental VDE values of Au_n^- and Au_nO_2^- clusters are collected in Table 1. The values for all Au_n^-

Table 1. Calculated Vertical Detachment Energy VDE (eV) for Anionic Au_n^- and Au_nO_2^- Clusters, together with the Experimental Data for Comparison

cluster	VDE (eV)		cluster	VDE (eV)	
	theo.	exp.		theo.	exp.
Au_2^-	2.08	2.01 ^a	Au_2O_2^-	3.13	3.29 ^b
Au_3^-	3.68	3.88 ^a	Au_3O_2^-	3.68	3.90 ^b
Au_4^-	2.85	2.75 ^a	Au_4O_2^-	3.66	3.78 ^b
Au_5^-	3.17	3.09 ^a	Au_5O_2^-	3.27	3.15 ^b
Au_6^-	2.20	2.13 ^a	Au_6O_2^-	3.26	3.40 ^c
Au_7^-	3.52	3.46 ^a	Au_7O_2^-	3.49	3.45 ^b
Au_8^-	2.82	2.79 ^a	Au_8O_2^-	4.00	4.00 ^c
Au_9^-	3.95	3.83 ^a	Au_9O_2^-	4.01	
Au_{10}^-	4.09	3.91 ^a	$\text{Au}_{10}\text{O}_2^-$	4.06	3.90 ^d

^aReference 63. ^bReference 22. ^cReference 23. ^dReference 65.

clusters agree very well with the experimental data, and all differences are within 0.20 eV. These observations suggest that the structures of Au_n^- clusters obtained here are the true minima structures.

Compared to the PES of the Au_n^- clusters, the PESs of Au_nO_2^- clusters contain substantially more peaks, as seen in Figure 4. In the simulated PES of Au_2O_2^- , there are six obvious peaks, with the first peak located around 3.13 eV. This onset and the increase in spectral strength around 5 eV agree very

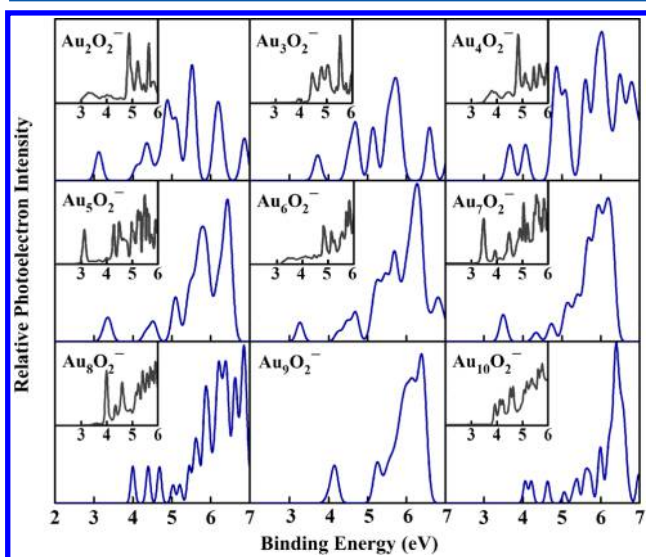


Figure 4. Calculated photoelectron spectra of Au_nO_2^- ($n = 2-10$) clusters, along with the available experimental data [$(n = 2-5$ and 7),²² ($n = 6$ and 8),²³ and ($n = 10$)⁶⁵] for comparison. The blue curves show the theoretical results, while the gray curves represent the experimental results.

well with the experimental data. In the experimental PES of Au_3O_2^- , there is a very small peak around 3.90 eV, close to the first peak of pure Au_3^- , which suggests that this peak originates from a physisorbed $\text{Au}_3^-(\text{O}_2)$ species.²² In agreement with this, the simulated PES of the Au_3O_2^- cluster shows five major peaks with a first peak corresponding to a VDE of 3.90 eV, in accordance with the physisorption picture. For Au_4O_2^- , ignoring the relative intensities of the peaks, the peak structure and positions are similar to the experimental data. For $n = 5$ and 7 , there are fewer features in the simulated spectra compared to the experimental results. There is also a missing feature between 3.50 and 4.00 eV in the PES of Au_6O_2^- . For Au_8O_2^- and $\text{Au}_{10}\text{O}_2^-$, the shapes and the positions of the first peak coincide with the experimental data. Summarized in Table 1, we conclude that the theoretical VDE values of the Au_nO_2^- clusters agree well with the experimental values. Most differences are less than 0.20 eV, with a maximum of 0.22 eV for $n = 3$. As stated above for the anionic Au_n^- clusters, these results confirm that the lowest-energy structures obtained are true ground-state structures and provide further support to the accuracy of our calculations.

3.3. Relative Stabilities. As an effective criterion of the inherent stability of a cluster, the average binding energies (E_b) of the Au_nO_2^Q clusters as well as the Au_nO_2^Q ($n = 2-10$; $Q = 0, -1$) clusters are defined as follows:

$$E_b(\text{Au}_n\text{O}_2) = [nE(\text{Au}) + E(\text{O}_2) - E(\text{Au}_n\text{O}_2)] / (n + 2) \quad (1)$$

$$E_b(\text{Au}_n\text{O}_2^-) = [(n - 1)E(\text{Au}) + E(\text{Au}^-) + E(\text{O}_2) - E(\text{Au}_n\text{O}_2^-)] / (n + 2) \quad (2)$$

E is the total energy of the corresponding cluster or atom. Larger values of E_b represent stronger chemical stability. To facilitate comparison across the clusters, the binding energies for the Au_nO_2^Q ($n = 2-10$; $Q = 0, -1$) clusters are plotted in Figure 5a, with the corresponding values summarized in Table

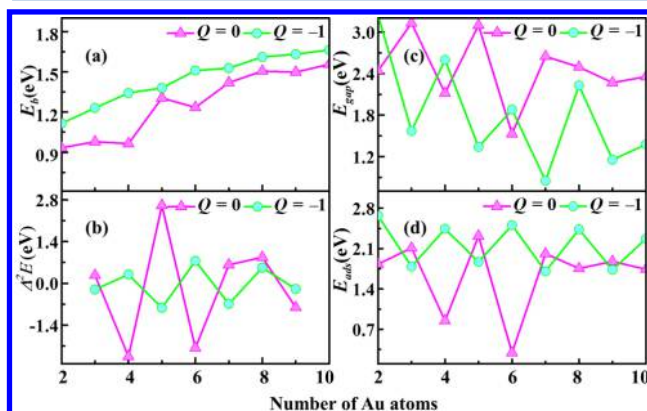


Figure 5. Size dependence of (a) the averaged binding energies E_b and (b) second-order energy differences Δ^2E , (c) HOMO-LUMO energy gaps E_{gap} , and (d) absolute value of the adsorption energy E_{ads} for the lowest energy Au_nO_2^Q ($n = 2-10$; $Q = 0, -1$) clusters.

2. From this figure, we can see that all neutral Au_nO_2 clusters have lower binding energies than their anionic counterparts, and E_b of the Au_nO_2^Q ($n = 2-10$; $Q = 0, -1$) clusters generally increases with cluster size. As an obvious outlier from a mostly linear trend, Au_5O_2 can be considered as a local optimum.

Table 2. Calculated Electronic States, Symmetries, Averaged Binding Energies E_b (eV), and HOMO–LUMO Energy Gaps E_{gap} (eV) for the Ground-State Au_nO_2^Q ($n = 2–10$, $Q = 0, -1$) Clusters

n	Au_nO_2				Au_nO_2^-			
	sta.	sym.	E_b	E_{gap}	sta.	sym.	E_b	E_{gap}
2	$^3\text{A}''$	C_s	0.93	2.44	$^2\text{A}''$	C_s	1.12	3.31
3	$^2\text{A}_2$	C_{2v}	0.98	3.13	^3A	C_1	1.23	1.57
4	$^1\text{A}'$	C_s	0.96	2.12	^2A	C_1	1.34	2.60
5	$^2\text{A}_2$	C_{2v}	1.30	3.10	^3A	C_1	1.38	1.34
6	^1A	C_1	1.23	1.53	^2A	C_s	1.51	1.88
7	^2A	C_1	1.41	2.65	^3A	C_1	1.53	0.85
8	$^3\text{A}''$	C_s	1.51	2.49	^2A	C_1	1.61	2.23
9	^2A	C_1	1.50	2.27	$^3\text{A}''$	C_s	1.63	1.16
10	^3A	C_1	1.56	3.36	^2A	C_1	1.66	1.38

A more sensitive quantity reflecting the relative stability of clusters, the second-order differences of the energy (Δ^2E) are calculated for all Au_nO_2^Q ($Q = 0, -1$) clusters as

$$\Delta^2E(\text{Au}_n\text{O}_2) = E(\text{Au}_{n-1}\text{O}_2) + E(\text{Au}_{n+1}\text{O}_2) - 2E(\text{Au}_n\text{O}_2) \quad (3)$$

$$\Delta^2E(\text{Au}_n\text{O}_2^-) = E(\text{Au}_{n-1}\text{O}_2^-) + E(\text{Au}_{n+1}\text{O}_2^-) - 2E(\text{Au}_n\text{O}_2^-) \quad (4)$$

Figure 5b shows the size dependence of Δ^2E for the Au_nO_2^Q ($n = 2–10$; $Q = 0, -1$) clusters. For the neutral clusters, two distinct peaks are found at $n = 3$ and 5 , indicating that the clusters Au_3O_2 and Au_5O_2 are more stable than their neighbors. For the anionic species, there is an obvious odd–even oscillation, a phenomenon corroborating that Au_nO_2 clusters with even n are more stable than those with odd n .

The HOMO–LUMO energy gap (E_{gap}) is a reflection of the energy cost for an electronic excitation from the highest occupied molecular orbital (HOMO) to the lowest unoccupied molecular orbital (LUMO), and thus serves as further support to the stability of a cluster. A large E_{gap} often tends to correlate with remarkable chemical stability. We have calculated the E_{gap} values for the neutral and anionic Au_nO_2 clusters and summarize them in Table 2. Figure 5c gives the E_{gap} values of Au_nO_2^Q ($Q = 0, -1$) clusters as functions of cluster size. The trend for the anionic clusters shows the standard even–odd oscillation behavior. For anionic Au_nO_2^- clusters, four local maxima E_{gap} values of 3.24, 2.60, 1.88, and 2.23 eV are found at $n = 2, 4, 6$, and 8 , respectively. Correspondingly, the Au_nO_2^- ($n = 3, 5, 7, 9$) are less stable, which agrees with the results of Δ^2E . As for the neutral Au_nO_2 clusters, there are three obvious peaks for $n = 3, 5$, and 7 , which suggests that the Au_nO_2 ($n = 3, 5$, and 7) clusters possess stronger chemical stability than their neighbors. The most stable anionic clusters $\text{Au}_{2/4/6}\text{O}_2^-$ even exhibit larger band gaps than their neutral counterparts, assisted by acquisition of the additional electron.

Au_nO_2^- clusters with even n are molecularly chemisorbed complexes, and Au_nO_2^- clusters with odd n can be seen as weakly bonded van der Waals complexes. The molecularly chemisorbed complexes are more stable than the weakly bonded van der Waals complexes. For neutral clusters, the even/odd argument should be reversed, and the conclusions of the stability analysis above indicate indeed that Au_3O_2 , Au_5O_2 , and Au_7O_2 clusters have a great chance to be chemical adsorption products. The neutral Au_5O_2 cluster is the most

promising among these. It is worth noting that our results generally fit well with earlier conclusions²⁹ that O_2 binds more strongly to clusters with an odd number of electrons than with an even number.

3.4. Adsorption Analysis. Based on the optimized geometries, we have calculated the natural charges of the oxygen molecule and the adsorption energy of O_2 on Au clusters, which is defined as the energy difference between the adsorption system with the individual cluster and oxygen molecule:

$$E_{\text{ads}}(\text{Au}_n\text{O}_2^Q) = E(\text{Au}_n\text{O}_2^Q) - E(\text{Au}_n^Q) - E(\text{O}_2), \quad Q = 0, -1 \quad (5)$$

E_{ads} is the adsorption energy of the corresponding cluster. The results of both E_{ads} and natural charges of the oxygen molecule are summarized in Table 3. By construction, the more negative

Table 3. Adsorption Energy E_{ads} (eV) of the Oxygen Molecule and the Natural Charges of O_2 NC(O_2) in the Ground-State Au_nO_2^Q ($Q = 0, -1$) Clusters

n	Au_nO_2		Au_nO_2^-	
	E_{ads}	NC(O_2)	E_{ads}	NC(O_2)
2	-1.83	0.00	-2.67	-0.65
3	-2.11	-0.42	-1.79	-0.17
4	-0.85	-0.44	-2.44	-0.59
5	-2.32	-0.53	-1.87	-0.33
6	-0.29	-0.20	-2.51	-0.65
7	-2.01	-0.53	-1.70	-0.20
8	-1.75	0.02	-2.43	-0.58
9	-1.88	-0.17	-1.73	-0.21
10	-1.74	0.02	-2.27	-0.56

the adsorption energy, the more stable the corresponding adsorption reactions. For better observation, we have plotted the absolute value of adsorption energy in Figure 5d for all Au_nO_2^Q clusters. The adsorption energy of the Au_nO_2^- clusters reveals the even–odd oscillation behavior, which again highlights the conclusion that small gold cluster anions with even-numbered atoms can molecularly chemisorb O_2 , whereas clusters with odd-numbered atoms are inert toward O_2 .²³ The results of natural charges of O_2 in anionic clusters are in line with this conclusion. From Table 3, we can see that the charges of O_2 are always negative and the absolute value of the charges are much larger for even n than for odd n , which shows the more significant charge transfer from the parent Au_n^- cluster to the oxygen molecule. The anion species are better electron donors than the corresponding neutral species, because the electron affinities are always smaller than ionization potentials.²⁹ Thus, the Au_nO_2^- clusters with even-number n have larger absolute values of adsorption energies. For neutral Au_nO_2 clusters, the absolute value of adsorption energy of Au_nO_2 with $n = 3, 5$, and 7 is relatively larger than those of their adjacent neutral clusters. This is consistent with the conclusion that Au_n clusters with an odd number of electrons hold the promise of chemisorbing an O_2 molecule, for charges transferring from Au_n to O_2 is the dominant mechanism of the chemisorption process.⁶⁶ Correspondingly, the natural charges of the oxygen molecule in Au_nO_2 clusters with $n = 3, 5$, and 7 have the largest absolute values (with the exception of $n = 4$). The large charge transfer in the Au_4O_2 cluster is probably due to its special geometry and oxygen binding motif, and since it does not

possess a high negative value of adsorption energy or high inherent stability, we will not analyze it in detail here. The large negative values of the natural charges of O_2 of Au_nO_2 clusters with $n = 3, 5,$ and 7 give confidence to the conclusion that O_2 is chemisorbed onto the parent Au_n cluster. Using the relatively large absolute values of adsorption energies as a criterion to indicate the chemisorption of O_2 molecules, these results give further support to the assumption that O_2 molecules can be chemisorbed onto neutral Au_n clusters, especially in the case of Au_5O_2 , which possesses the largest absolute value of adsorption energy.

3.5. Chemical Bonding Analysis. According to the analysis above, the neutral Au_5O_2 cluster exhibits an unexpected stability along with a large absolute value of adsorption energy and charge transfer and can therefore be regarded as the most promising candidate of chemisorption between neutral Au_n clusters and a O_2 molecule. To gain insight into its bonding properties, the corresponding molecular orbitals (MO) of Au_5O_2 were analyzed and are presented in Figure 6. Despite

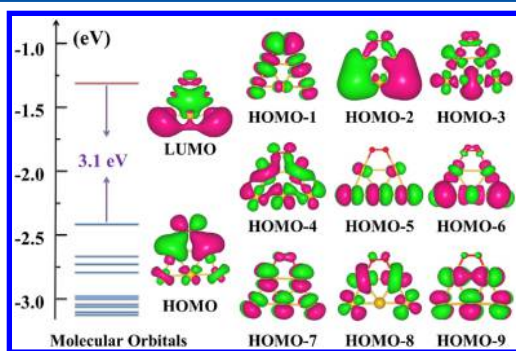


Figure 6. Molecular orbitals and energy levels of the neutral Au_5O_2 cluster.

their different shapes, they are combinations of two sets of atomic orbitals: mostly d-type Au orbitals and p-type O orbitals. For the LUMO, the bottom two Au atoms possess s-type character, and there is a strong Au–Au bond over two of the middle three Au atoms. For the occupied MOs HOMO, HOMO–2, and HOMO–4, the $O p_z$ orbitals (taken as in-plane) interact with the Au $5d_z^2$ orbitals to form Au–O σ bonding. The HOMO– n for $n = 1, 7,$ and 9 involve the same d_{yz} and d_{xy} atomic orbitals of Au atoms and the p_y atomic orbital (taken as out-of-plane) of the O atomic orbitals, while the HOMO–5 is formed primarily by d_{xy} orbitals of Au atoms. The remaining MOs shown involve bonding and antibonding combinations with the $O p_z$ atomic orbitals. The Au–Au interaction (mainly the interactions of the d orbitals) of the HOMO–2, HOMO–4, and HOMO–6 contribute to the stability of the C_{2v} structure. On the basis of the MO configuration, the Au_5O_2 cluster possesses two σ bonds and one antibonding π^* bond (HOMO–1) between Au and O atoms, because one of the three σ bonds and the antibonding σ^* bond (HOMO–8) cancel each other. These molecular orbitals indicate that there are strong interactions in the cyclic arrangement between the O atoms and the Au atoms they are bound to.

To improve our understanding of the bonding properties in the Au_5O_2 cluster further, we performed a chemical bonding analysis using the AdNDP approach, which is a visual and efficient algorithm to interpret the nature of molecular orbitals. The AdNDP approach obtains electron pairs by partitioning

the electron density matrix into $nc-2e$ terms (n ranges from 1 to the maximum number of atoms in the system), and the electron pair serves as a unit to describe the chemical bonding. Figure 7 gives the representative results of AdNDP for Au_5O_2

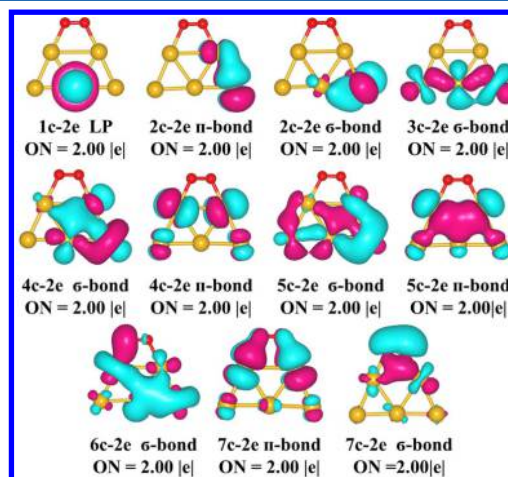


Figure 7. AdNDP chemical bonding analysis of the neutral Au_5O_2 cluster. LP represents lone pair localized bond. ON stands for the occupation number.

(the remaining can be seen in the Supporting Information, Figure S1), and the following discussion is about the revealed chemical bonds. The occupation numbers (ONs) of all chemical bonds maintain the ideal values $2.00 |e|$, which is an illustration of the validity of the AdNDP analysis we obtained. There are two kinds of localized $2c-2e$ bonds: one Au–Au σ bond and one Au–Au π bond. The rest of the valence electron density is, except for one lone pair (LP), totally delocalized. There are five delocalized σ bonds and three delocalized π bonds (only considering the representative results). Except for the $6c-2e$ σ bond, $7c-2e$ σ bond, and $7c-2e$ π bond shown in the bottom row of Figure 7, the remaining delocalized bonds describe the chemical bonding among Au atoms only. The $6c-2e$ σ bond, $7c-2e$ σ bond, and $7c-2e$ π bond then visualize the strong bond between Au and O atoms, which make the C_{2v} structure of Au_5O_2 so stable. Accordingly, the Au_5O_2 cluster does not exist in the form of a weakly bonded van der Waals complex but a chemisorbed complex for the strong interactions between O and Au atoms.

4. CONCLUSIONS

In summary, we have reported a detailed investigation of the neutral and anionic Au_n^Q and $Au_nO_2^Q$ ($n = 2-10, Q = 0, -1$) clusters on the basis of the CALYPSO structure searching method and density functional theory. The ground-state structures of neutral and anionic Au_n clusters are planar, and there are two ways the oxygen molecule binds to the parent gold clusters. The reasonable agreement between our simulated photoelectron spectra and the experimental PES give forceful support that the ground-state structures we obtained are truly global minima. Based on the optimized geometries, we have calculated the inherent stability and the corresponding adsorption energies. The results showed that neutral gold clusters with an odd number of electrons bind O_2 more strongly, because the presence of an unpaired electron makes them better electron donors. Furthermore, the molecular orbital and chemical bonding analysis of the Au_5O_2 cluster

confirm the chemical adsorption of an oxygen molecule to a neutral gold cluster. We hope this work can provide the reference for further theoretical and experimental investigations of the adsorption behavior between O₂ and neutral gold clusters.

■ ASSOCIATED CONTENT

Supporting Information

The Supporting Information is available free of charge on the ACS Publications website at DOI: 10.1021/acs.jpcc.7b09022.

Electronic states, symmetries, average binding energies E_b , and HOMO–LUMO energy gaps E_{gap} of the ground-state Au_n cluster. (PDF)

■ AUTHOR INFORMATION

Corresponding Authors

*E-mail: scu_kuang@163.com.

*E-mail: lucheng@calypso.cn.

*E-mail: a.hermann@ed.ac.uk.

ORCID

Xiao Yu Kuang: 0000-0001-7489-9715

Cheng Lu: 0000-0003-1746-7697

Notes

The authors declare no competing financial interest.

■ ACKNOWLEDGMENTS

This work was supported by the National Natural Science Foundation of China (Nos. 11574220, 11304167, and 21671114), the 973 Program of China (No. 2014CB660804), the Special Program for Applied Research on Super Computation of the NSFC-Guangdong Joint Fund (the second phase) under Grant No. U1501501, and the Program for Science & Technology Innovation Talents in Universities of Henan Province (No. 15HASTIT020). Parts of the calculations were performed using the Cherry Creek Supercomputer of the UNLV's National Supercomputing Institute.

■ REFERENCES

- (1) Kröger, H.; Gerhards, I.; Milinović, V.; Reinke, P. Synthesis of Au–C₆₀ Cluster Materials. *J. Phys. Chem. C* **2007**, *111*, 10170–10174.
- (2) Radziuk, D.; Shchukin, D.; Möhwald, H. Sonochemical Design of Engineered Gold–Silver Nanoparticles. *J. Phys. Chem. C* **2008**, *112*, 2462–2468.
- (3) Radziuk, D.; Grigoriev, D.; Zhang, W.; Su, D. S.; Möhwald, H.; Shchukin, D. Ultrasound-Assisted Fusion of Preformed Gold Nanoparticles. *J. Phys. Chem. C* **2010**, *114*, 1835–1843.
- (4) Li, J.; Li, X.; Zhai, H. J.; Wang, L. S. Au₂₀: A Tetrahedral Cluster. *Science* **2003**, *299*, 864–867.
- (5) Huang, W.; Wang, L. S. Probing the 2D to 3D Structural Transition in Gold Cluster Anions Using Argon Tagging. *Phys. Rev. Lett.* **2009**, *102*, 153401.
- (6) Hermann, A.; Derzsi, M.; Grochala, W.; Hoffmann, R. AuO: Evolving from Dis- to Comproportionation and Back Again. *Inorg. Chem.* **2016**, *55*, 1278–1286.
- (7) Shi, H.; Asahi, R.; Stampfl, C. Properties of the gold oxides Au₂O₃ and Au₂O: First-principles investigation. *Phys. Rev. B: Condens. Matter Mater. Phys.* **2007**, *75*, 205125.
- (8) Haruta, M.; Yamada, N.; Kobayashi, T.; Iijima, S. Gold Catalysts Prepared by Coprecipitation for Low-Temperature Oxidation of Hydrogen and of Carbon Monoxide. *J. Catal.* **1989**, *115*, 301–309.
- (9) Valden, M.; Lai, X.; Goodman, D. W. Onset of Catalytic Activity of Gold Clusters on Titania with the Appearance of Nonmetallic Properties. *Science* **1998**, *281*, 1647–1650.

(10) Xu, C.; Su, J.; Xu, X.; Liu, P.; Zhao, H.; Tian, F.; Ding, Y. Low Temperature CO Oxidation over Unsupported Nanoporous Gold. *J. Am. Chem. Soc.* **2007**, *129*, 42–43.

(11) Socaciu, L. D.; Hagen, J.; Bernhardt, T. M.; Wöste, L.; Heiz, U.; Häkkinen, H.; Landman, U. Catalytic CO Oxidation by Free Au₂[−]: Experiment and Theory. *J. Am. Chem. Soc.* **2003**, *125*, 10437–10445.

(12) Hayashi, T.; Tanaka, K.; Haruta, M. Selective Vapor-Phase Epoxidation of Propylene over Au/TiO₂ Catalysts in the Presence of Oxygen and Hydrogen. *J. Catal.* **1998**, *178*, 566–575.

(13) Zalc, J. M.; Sokolovskii, V.; Löffler, D. G. Are Noble Metal-Based Water-Gas Shift Catalysts Practical for Automotive Fuel Processing? *J. Catal.* **2002**, *206*, 169–171.

(14) Liu, Z. P.; Jenkins, S. J.; King, D. A. Origin and Activity of Oxidized Gold in Water-Gas-Shift Catalysis. *Phys. Rev. Lett.* **2005**, *94*, 196102.

(15) Jia, J.; Haraki, K.; Kondo, J. N.; Domen, K.; Tamaru, K. Selective Hydrogenation of Acetylene over Au/Al₂O₃ Catalyst. *J. Phys. Chem. B* **2000**, *104*, 11153–11156.

(16) Okumura, M.; Kitagawa, Y.; Haruta, M.; Yamaguchi, K. DFT studies of interaction between O₂ and Au cluster. The role of anionic surface Au atoms on Au clusters for catalyzed oxygenation. *Chem. Phys. Lett.* **2001**, *346*, 163–168.

(17) Kim, Y. D.; Fischer, M.; Ganteför, G. Origin of unusual catalytic activities of Au-based catalysts. *Chem. Phys. Lett.* **2003**, *377*, 170–176.

(18) Stolcic, D.; Fischer, M.; Ganteför, G.; Kim, Y. D.; Sun, Q.; Jena, P. Direct Observation of Key Reaction Intermediates on Gold Clusters. *J. Am. Chem. Soc.* **2003**, *125*, 2848–2849.

(19) Ding, X.; Li, Z.; Yang, J.; Hou, J. G.; Zhu, Q. Adsorption energies of molecular oxygen on Au clusters. *J. Chem. Phys.* **2004**, *120*, 9594–9600.

(20) Ding, X.; Dai, B.; Yang, J.; Hou, J. G.; Zhu, Q. Assignment of photoelectron spectra of Au_nO₂[−] (n = 2,4,6) clusters. *J. Chem. Phys.* **2004**, *121*, 621–623.

(21) Molina, L. M.; Hammer, B. Oxygen adsorption at anionic free and supported Au clusters. *J. Chem. Phys.* **2005**, *123*, 161104.

(22) Huang, W.; Zhai, H. J.; Wang, L. S. Probing the Interactions of O₂ with Small Gold Cluster Anions (Au_n[−], n = 1–7): Chemisorption vs Physisorption. *J. Am. Chem. Soc.* **2010**, *132*, 4344–4351.

(23) Pal, R.; Wang, L. M.; Pei, Y.; Wang, L. S.; Zeng, X. C. Unraveling the Mechanisms of O₂ Activation by Size-Selected Gold Clusters: Transition from Superoxo to Peroxo Chemisorption. *J. Am. Chem. Soc.* **2012**, *134*, 9438–9445.

(24) Lee, H. M.; Lee, K. H.; Lee, G.; Kim, K. S. Geometrical and Electronic Characteristics of Au_nO₂[−] (n = 2–7). *J. Phys. Chem. C* **2015**, *119*, 14383–14391.

(25) Haruta, M.; Tsubota, S.; Kobayashi, T.; Kageyama, H.; Genet, M. J.; Delmon, B. Low-Temperature Oxidation of CO over Gold Supported on TiO₂, α-Fe₂O₃, and Co₃O₄. *J. Catal.* **1993**, *144*, 175–192.

(26) Yoon, B.; Häkkinen, H.; Landman, U. Interaction of O₂ with Gold Clusters: Molecular and Dissociative Adsorption. *J. Phys. Chem. A* **2003**, *107*, 4066–4071.

(27) Sun, Q.; Jena, P.; Kim, Y. D.; Fischer, M.; Ganteför, G. Interactions of Au cluster anions with oxygen. *J. Chem. Phys.* **2004**, *120*, 6510–6515.

(28) Varganov, S. A.; Olson, R. M.; Gordon, M. S.; Metiu, H. The interaction of oxygen with small gold clusters. *J. Chem. Phys.* **2003**, *119*, 2531–2537.

(29) Mills, G.; Gordon, M. S.; Metiu, H. The adsorption of molecular oxygen on neutral and negative Au_n clusters (n = 2–5). *Chem. Phys. Lett.* **2002**, *359*, 493–499.

(30) Woodham, A. P.; Meijer, G.; Fielicke, A. Charge Separation Promoted Activation of Molecular Oxygen by Neutral Gold Clusters. *J. Am. Chem. Soc.* **2013**, *135*, 1727–1730.

(31) Gao, M.; Horita, D.; Ono, Y.; Lyalin, A.; Maeda, S.; Taketsugu, T. Isomerization in Gold Clusters upon O₂ Adsorption. *J. Phys. Chem. C* **2017**, *121*, 2661–2668.

- (32) Zhu, L.; Wang, H.; Wang, Y. C.; Lv, J.; Ma, Y. M.; Cui, Q. L.; Ma, Y. M.; Zou, G. T. Substitutional Alloy of Bi and Te at High Pressure. *Phys. Rev. Lett.* **2011**, *106*, 145501.
- (33) Lv, J.; Wang, Y. C.; Zhu, L.; Ma, Y. M. Predicted Novel High-Pressure Phases of Lithium. *Phys. Rev. Lett.* **2011**, *106*, 015503.
- (34) Wang, H.; Tse, J. S.; Tanaka, K.; Iitaka, T.; Ma, Y. M. Superconductive sodalite-like clathrate calcium hydride at high pressures. *Proc. Natl. Acad. Sci. U. S. A.* **2012**, *109*, 6463–6466.
- (35) Li, Y. W.; Hao, J.; Liu, H. Y.; Li, Y. L.; Ma, Y. M. The metallization and superconductivity of dense hydrogen sulfide. *J. Chem. Phys.* **2014**, *140*, 174712.
- (36) Zhu, L.; Liu, H. Y.; Pickard, C. J.; Zou, G. T.; Ma, Y. M. Reactions of xenon with iron and nickel are predicted in the Earth's inner core. *Nat. Chem.* **2014**, *6*, 644–648.
- (37) Jin, Y. Y.; Maroulis, G.; Kuang, X. Y.; Ding, L. P.; Lu, C.; Wang, J. J.; Lv, J.; Zhang, C. Z.; Ju, M. Geometries, stabilities and fragmental channels of neutral and charged sulfur clusters: S_n^Q ($n = 3–20$, $Q = 0, \pm 1$). *Phys. Chem. Chem. Phys.* **2015**, *17*, 13590–13597.
- (38) Xing, X. D.; Hermann, A.; Kuang, X. Y.; Ju, M.; Lu, C.; Jin, Y. Y.; Xia, X. X.; Maroulis, G. Insights into the geometries, electronic and magnetic properties of neutral and charged palladium clusters. *Sci. Rep.* **2016**, *6*, 19656.
- (39) Lv, J.; Wang, Y. C.; Zhu, L.; Ma, Y. M. Particle-swarm structure prediction on clusters. *J. Chem. Phys.* **2012**, *137*, 084104.
- (40) Wang, Y. C.; Lv, J.; Zhu, L.; Ma, Y. M. CALYPSO: A method for crystal structure prediction. *Comput. Phys. Commun.* **2012**, *183*, 2063–2070.
- (41) Wang, Y. C.; Lv, J.; Zhu, L.; Ma, Y. M. Crystal structure prediction via particle-swarm optimization. *Phys. Rev. B: Condens. Matter Mater. Phys.* **2010**, *82*, 094116.
- (42) Frisch, M.; et al. *Gaussian 09*; Gaussian, Inc.: Wallingford, CT, 2009.
- (43) Becke, A. D. Density-functional thermochemistry. III. The role of exact exchange. *J. Chem. Phys.* **1993**, *98*, 5648–5652.
- (44) Perdew, J. P.; Wang, Y. Pair-distribution function and its coupling-constant average for the spin-polarized electron gas. *Phys. Rev. B: Condens. Matter Mater. Phys.* **1992**, *46*, 12947–12954.
- (45) Hay, P. J.; Wadt, W. R. Ab initio effective core potentials for molecular calculations. Potentials for K to Au including the outermost core orbitals. *J. Chem. Phys.* **1985**, *82*, 299–310.
- (46) McLean, A. D.; Chandler, G. S. Contracted Gaussian basis sets for molecular calculations. I. Second row atoms, $Z = 11–18$. *J. Chem. Phys.* **1980**, *72*, 5639–5648.
- (47) Casida, M. E.; Jamorski, C.; Casida, K. C.; Salahub, D. R. Molecular excitation energies to high-lying bound states from time-dependent density functional response theory: Characterization and correction of the time-dependent local density approximation ionization threshold. *J. Chem. Phys.* **1998**, *108*, 4439–4449.
- (48) Zubarev, D. Y.; Boldyrev, A. I. Developing paradigms of chemical bonding: adaptive natural density partitioning. *Phys. Chem. Chem. Phys.* **2008**, *10*, 5207–5217.
- (49) Lu, T.; Chen, F. Multiwfn: A Multifunctional Wavefunction Analyzer. *J. Comput. Chem.* **2012**, *33*, 580–590.
- (50) Majumder, C. Effect of Si adsorption on the atomic and electronic structure of Au_n clusters ($n = 1–8$) and the Au (111) surface: First-principles calculations. *Phys. Rev. B: Condens. Matter Mater. Phys.* **2007**, *75*, 235409.
- (51) Schwerdtfeger, P.; Dolg, M.; Schwarz, W. H. E.; Bowmaker, G. A.; Boyd, P. D. W. Relativistic effects in gold chemistry. I. Diatomic gold compounds. *J. Chem. Phys.* **1989**, *91*, 1762–1774.
- (52) Häkkinen, H.; Landman, U. Gold clusters (Au_N , $2 \leq N \leq 10$) and their anions. *Phys. Rev. B: Condens. Matter Mater. Phys.* **2000**, *62*, R2287–R2290.
- (53) Olson, R. M.; Varganov, S.; Gordon, M. S.; Metiu, H.; Chretien, S.; Piecuch, P.; Kowalski, K.; Kucharski, S. A.; Musial, M. Where Does the Planar-to-Nonplanar Turnover Occur in Small Gold Clusters? *J. Am. Chem. Soc.* **2005**, *127*, 1049–1052.
- (54) Walker, A. V. Structure and energetics of small gold nanoclusters and their positive ions. *J. Chem. Phys.* **2005**, *122*, 094310.
- (55) Remacle, F.; Kryachko, E. S. Structure and energetics of two- and three-dimensional neutral, cationic, and anionic gold clusters $Au_{s \leq n \leq 9}^Z$ ($Z = 0, 1$). *J. Chem. Phys.* **2005**, *122*, 044304.
- (56) Castro, A.; Marques, M. A. L.; Romero, A. H.; Oliveira, M. J. T.; Rubio, A. The role of dimensionality on the quenching of spin-orbit effects in the optics of gold nanostructures. *J. Chem. Phys.* **2008**, *129*, 144110.
- (57) Assadollahzadeh, B.; Schwerdtfeger, P. A systematic search for minimum structures of small gold clusters Au_n ($n = 2–20$) and their electronic properties. *J. Chem. Phys.* **2009**, *131*, 064306.
- (58) Serapian, S. A.; Bearpark, M. J.; Bresme, F. The shape of Au_8 : gold leaf or gold nugget? *Nanoscale* **2013**, *5*, 6445–6457.
- (59) Götz, D. A.; Schäfer, R.; Schwerdtfeger, P. The Performance of Density Functional and Wavefunction-Based Methods for 2D and 3D Structures of Au_{10} . *J. Comput. Chem.* **2013**, *34*, 1975–1981.
- (60) Hansen, J. A.; Piecuch, P.; Levine, B. G. Communication: Determining the lowest-energy isomer of Au_8 : 2D, or not 2D. *J. Chem. Phys.* **2013**, *139*, 091101.
- (61) Johansson, M. P.; Warnke, I.; Le, A.; Furche, F. At What Size do Neutral Gold Clusters Turn Three-Dimensional? *J. Phys. Chem. C* **2014**, *118*, 29370–29377.
- (62) Lee, H. M.; Ge, M.; Sahu, B. R.; Tarakeshwar, P.; Kim, K. S. Geometrical and Electronic Structures of Gold, Silver, and Gold-Silver Binary Clusters: Origins of Ductility of Gold and Gold-Silver Alloy Formation. *J. Phys. Chem. B* **2003**, *107*, 9994–10005.
- (63) Häkkinen, H.; Yoon, B.; Landman, U.; Li, X.; Zhai, H. J.; Wang, L. S. On the Electronic and Atomic Structures of Small Au_N^- ($N = 4–14$) Clusters: A Photoelectron Spectroscopy and Density-Functional Study. *J. Phys. Chem. A* **2003**, *107*, 6168–6175.
- (64) Liu, Z.; Qin, Z.; Xie, H.; Cong, R.; Wu, X.; Tang, Z. Structure of $Au_4^{0/-1}$ in the gas phase: A joint geometry relaxed ab initio calculations and vibrationally resolved photoelectron imaging investigation. *J. Chem. Phys.* **2013**, *139*, 094306.
- (65) Huang, W.; Wang, L. S. Au_{10}^- : isomerism and structure-dependent O_2 reactivity. *Phys. Chem. Chem. Phys.* **2009**, *11*, 2663–2667.
- (66) Salisbury, B. E.; Wallace, W. T.; Whetten, R. L. Low-temperature activation of molecular oxygen by gold clusters: a stoichiometric process correlated to electron affinity. *Chem. Phys.* **2000**, *262*, 131–141.